

## Campigliaite, $\text{Cu}_4\text{Mn}(\text{SO}_4)_2(\text{OH})_6 \cdot 4\text{H}_2\text{O}$ , a new mineral from Campiglia Marittima, Tuscany, Italy

### I. Occurrence and description

SILVIO MENCHETTI AND Cesare SABELLI

CNR Centro di Studio per la Mineralogia e la Geochimica dei sedimenti  
Istituto di Mineralogia dell'Università  
Via La Pira 4, 50121, Firenze, Italy

#### Abstract

Campigliaite, a new copper and manganese sulfate mineral, occurs as tufts of light blue crystals in the sulfide ore bodies of Temperino mine, Campiglia Marittima, Tuscany, Italy. It is monoclinic, space group  $C2$ , with  $a = 21.707$ ,  $b = 6.098$ ,  $c = 11.245 \text{ \AA}$ ,  $\beta = 100.3^\circ$ . The tiny crystals, elongated [010] and flattened {100}, are always twinned (100). The calculated density is  $3.06 \text{ g cm}^{-3}$ . Optically it is biaxial (–) with  $\alpha = 1.589$ ,  $\beta = 1.645$ ,  $\gamma = 1.659$ . The strongest lines in the X-ray powder pattern are  $10.68(100)(200)$ ,  $5.34(60)(400)$ ,  $3.56(44)(600)$ ,  $2.673(5)(022 \text{ and } 800)$ .

The structure was solved using 689 independent reflections and refined to an  $R$  value of 0.124. The dominant structural feature is the arrangement of copper–oxygen polyhedra into dense sheets, parallel to (100). The sulfate groups are linked by a corner to both sides of sheets. The Mn atom coordinates four water molecules and two oxygen atoms of sulfate groups belonging to the same Cu–O–S layer. Subsequent layers are connected to each other by hydrogen bonds. The relationship between the structures of campigliaite and devillite and serpierite is discussed.

#### Introduction

In a previous paper (Conticini *et al.*, 1980) dealing with the alteration minerals from Campiglia Marittima (Tuscany, Italy) we briefly described a mineral, a hydrated basic sulfate of copper and manganese, which appeared to be different from any known sulfate. Further study revealed the mineral in question to be a new species.

The mineral,  $\text{Cu}_4\text{Mn}(\text{SO}_4)_2(\text{OH})_6 \cdot 4\text{H}_2\text{O}$ , is named campigliaite for the locality. Both the mineral and the name have been approved by the Commission on New Minerals and Mineral Names, IMA. A type specimen is deposited in the mineralogical Museum of Florence University (regional collection #214/I).

On the basis of the ideal formula, cell parameters and crystal structure, campigliaite is related to the serpierite–devillite series and, if one extra molecule of  $\text{H}_2\text{O}$  is neglected, it can be considered the manganese analogue of devillite.

#### Occurrence and paragenesis

The geographic location of Campiglia Marittima is depicted in Figure 1. A brief account of the

geology and ore deposits of the area is given in the above quoted paper, specially devoted to secondary minerals. The main tunnel of the third level of the “Miniera del Temperino” which goes from “Pozzo Earle” to “Pozzo Gowet” crosses through sulfide ore bodies (chalcopyrite, pyrite, sphalerite, galena, pyrrhotite, *etc.*). Starting from the point where the tunnel leaves the marblés and goes into the skarn, many copper oxysalts appear in the order: malachite, brochantite, antlerite, chalcantite. This sequence is related to the increasing acidity of solutions and the increasing concentration of  $\text{SO}_4$ . Serpierite also is common and widespread in the tunnel. However the most common and widespread secondary mineral is gypsum which occurs both as transparent crystals and as incrustations on other minerals. It is interesting to note that when two or more copper sulfates are present together, one can observe antlerite often grown on brochantite and chalcantite grown on antlerite.

Campigliaite was found only on the vugs of an ilvaite-rich skarn, collected in a side-tunnel (“galleria del fornello”) of the main tunnel. It occurs as



Fig. 1. Location map of the Campiglia Marittima mine, Tuscany, Italy.

tufted aggregates of tiny lath-like crystals (Fig. 2) of a pale blue color, associated with gypsum and sometimes with small amounts of brochantite and antlerite. Often campigliaite and gypsum are closely mixed; however campigliaite appears grown on gypsum crystals (Fig. 3). The genesis of campigliaite is probably related to the sulfate solutions formed by the oxidation of pyrite and other sulfide minerals. The presence of manganese in campigliaite is related to ilvaite. According to Rodolico (1931) ilvaite from Campiglia has 9.5% MnO which is a very high content for this mineral.

### Chemistry

Preliminary qualitative analyses of campigliaite, made with an ORTEC X-ray microanalyzer, revealed the presence of Cu, Mn, Zn, S and no other element with atomic number greater than 11. Many quantitative analyses were carried out by means of an ARL SEMQ electron microprobe using chalcopyrite, sphalerite and hortonolite as standards. It is important to note that these analyses were done under unfavorable conditions, since campigliaite crystals are very tiny and decompose under the electron beam. The average values of the three best analyses, MnO 9.95, CuO 40.60, ZnO 4.47, SO<sub>3</sub> 20.15, H<sub>2</sub>O 24.83% (by difference), correspond to

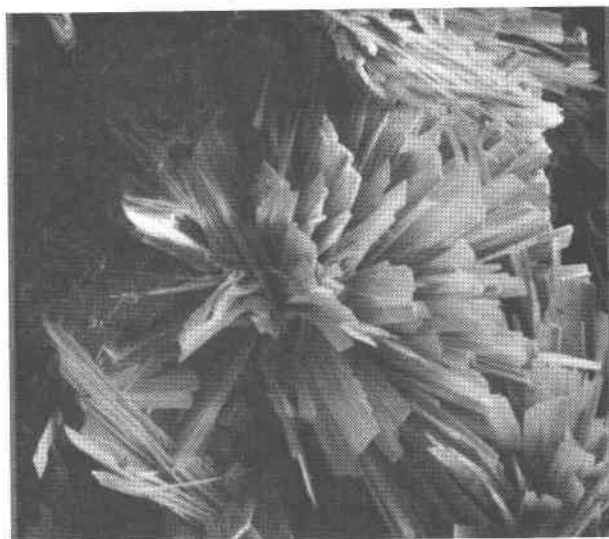


Fig. 2. Scanning electron photomicrograph of tufts of campigliaite. Crystals are about 0.2 mm long.

$\text{Mn}_{0.99}(\text{Cu}_{3.62}, \text{Zn}_{0.39})(\text{SO}_4)_{1.78}(\text{OH})_{6.44} \cdot 6.55\text{H}_2\text{O}$  on the basis of total metal = 5.

A wet chemical analysis, attempted on a small amount of purified material (less than 1 mg) confirmed the previous results for Mn, Cu and Zn (atomic absorption spectrometry). Unfortunately the scarceness of available material did not allow us to obtain reliable results for the SO<sub>4</sub> content. A TGA analysis, performed in order to obtain the H<sub>2</sub>O content, was also unsuccessful.



Fig. 3. Scanning electron photomicrograph of crystals of campigliaite grown on gypsum. Crystals are about 0.2 mm long.

The structural analysis yielded the formula  $\text{Mn}^{2+}\text{Cu}_4(\text{SO}_4)_2(\text{OH})_6 \cdot 4\text{H}_2\text{O}$ , where  $\text{Cu} = (\text{Cu}, \text{Zn})$ . This formula, which is somewhat different from the previous one, is supported by the density calculated from the Gladstone–Dale relationship. This ideal formula requires  $\text{MnO}$  10.50,  $\text{CuO}$  47.11,  $\text{SO}_3$  23.71,  $\text{H}_2\text{O}$  18.68%.

Campigliaite is slowly soluble in acetic acid without evident effervescence, suggesting the absence of  $\text{CO}_3$ .

### X-ray crystallography

X-ray single crystal study (Weissenberg camera and single-crystal diffractometer) revealed all crystals tested to be twinned with (100) as the twin plane. Campigliaite is monoclinic with Laue symmetry  $2/m$ . Space groups consistent with the observed systematic extinctions are  $C2/m$ ,  $Cm$  and  $C2$ , the latter being the one favored by the structural analysis.

The X-ray powder diffraction pattern, given in Table 1, was obtained by means of a Philips diffractometer, with  $\text{CoK}\alpha$  radiation,  $\text{NaF}$  as internal standard,  $1/4^\circ$   $2\theta$  per minute. Indexing was performed on the basis of lattice parameters determined on the single-crystal diffractometer and taking into account the intensities of reflections collected for the structural study. In this powder pattern only three reflections have relative intensities greater than 5. Moreover all three of these reflections belong to the  $h00$  series. This depends on the crystal structure and on a strong enhancement of intensities due to a preferred orientation caused by the  $\{100\}$  cleavage. Keeping this in mind there is a similarity evident between the powder patterns of campigliaite and serpierite and devillite (Faraone *et al.*, 1967). In the serpierite and devillite patterns are many lines which are not present in the campigliaite pattern; however the three stronger lines ( $h00$  series) are closely related. A slight similarity is also found with the pattern quoted by JCPDS for the mineral woodwardite from Carnarvonshire, Wales (card no. 17-132). No other similarities can be found; actually the chemical formula of woodwardite, which is a hydrated sulfate of  $\text{Cu}$  and  $\text{Al}$ , is uncertain, while lattice parameters, space group and crystal structure are unknown. According to Nickel (1976) the name "woodwardite" for the Welsh material is not correct in that this species is different from the woodwardite from Cornwall which is its type locality.

The lattice parameters of campigliaite, deter-

Table 1. X-ray powder pattern of campigliaite

h	k	l	d (calc)	d (obs)	I/I <sub>0</sub>
2	0	0	10.678	10.68	100
4	0	0	5.339	5.34	60
-4	0	2	4.239	4.26	1
-1	1	2	4.126	4.13	1
6	0	0	3.559	3.56	44
-6	0	2	3.272	3.28	1
0	0	4	2.766	2.768	2
0	2	2	2.670		
8	0	0	2.670 >	2.673	5
2	0	4	2.568	2.570	2
-4	2	2	2.475	2.478	1
4	0	4	2.294	2.295	1
10	0	0	2.136	2.137	1
12	0	0	1.780	1.781	2
-2	2	6	1.597	1.595	1
0	2	6	1.578	1.578	1
14	0	0	1.525 >	1.524	2
0	4	0	1.524 >		

mined by means of a least-squares calculation from powder data are:  $a = 21.707(1)$ ,  $b = 6.098(2)$ ,  $c = 11.245(1)\text{\AA}$ ,  $\beta = 100.3(1)^\circ$ .

### Physical properties and morphology

Crystals of campigliaite are transparent and light blue in color with vitreous luster. The perfect cleavage  $\{100\}$  is fully explained by the structure. The measured density, determined by the heavy-liquid method, reaches  $3.0\text{ g cm}^{-3}$ , but unfortunately this is an uncertain datum; because of the smallness of crystals, it was very difficult to determine when the mineral was suspended in the liquid. Calculated figures for the density are  $3.063\text{ g cm}^{-3}$  (normalized empirical formula with 7  $\text{H}_2\text{O}$  in total) and  $3.060\text{ g cm}^{-3}$  (Gladstone–Dale law on the same formula using the data of Mandarino, 1976). If 10  $\text{H}_2\text{O}$  are assumed, as directly derived from the analysis, the value of "Gladstone–Dale" density drops to  $2.93\text{ g cm}^{-3}$ . The density values of serpierite and devillite are very close to that of campigliaite (Table 2) and thus support the chemical formula of campigliaite derived from the structural analysis.

Under the microscope<sup>1</sup> the mineral appears in a pale greenish-blue color and without evident pleochroism. It is biaxial negative with refractive indices  $\alpha = 1.589$ ,  $\beta = 1.645$ ,  $\gamma = 1.659$ . The mean refractive index calculated from the Gladstone–Dale relationship, using the ideal chemical formula,

<sup>1</sup>Optical properties were wholly determined by Dr. N. Cipriani, University of Florence.

Table 2. Chemical composition and crystal data of campigliaite, devillite and serpierite

Campigliaite	Devillite	Serpierite
$\text{Cu}_4\text{Mn}(\text{SO}_4)_2(\text{OH})_6 \cdot 4\text{H}_2\text{O}$	$\text{Cu}_4\text{Ca}(\text{SO}_4)_2(\text{OH})_6 \cdot 3\text{H}_2\text{O}$	$(\text{Cu}, \text{Zn})_4\text{Ca}(\text{SO}_4)_2(\text{OH})_6 \cdot 3\text{H}_2\text{O}$
$a = 21.707\text{Å}$ Sp.gr. C2 $b = 6.098$ Z = 4 $c = 11.245$ $D_m \sim 3.00 \text{ g/cm}^3$ $\beta = 100.3^\circ$ $D_c = 3.06$ $v = 1464.5\text{Å}^3$	$a = 20.870\text{Å}$ Sp.gr. P2 <sub>1</sub> /c $b = 6.135$ Z = 8 $c = 22.191$ $D_m = 3.13 \text{ g/cm}^3 (+)$ $\beta = 102.73^\circ$ $D_c = 3.06$ $v = 2771.4\text{Å}^3$	$a = 22.186\text{Å}$ Sp.gr. C2/c $b = 6.250$ Z = 8 $c = 21.853$ $D_m = 3.07 \text{ g/cm}^3$ $\beta = 113.36^\circ$ $D_c = 3.08$ $v = 2781.8\text{Å}^3$
$X \sim a$ 1.589 2V = 52° $Y \sim c$ 1.645 ( - ) $Z = b$ 1.659 $r < v$ , weak	$X \wedge a \sim 13^\circ$ 1.585 2V = 39° $Y \sim c$ 1.649 ( - ) $Z = b$ 1.660 $r < v$ , marked (+)	$X \wedge a \sim 24^\circ$ 1.583 2V = 37° $Y = b$ 1.641 ( - ) $Z \sim c$ 1.648 $r > v$ , strong (+)

Data for devillite and serpierite from Faraone *et al.* (1967), except those with (+) from Palache *et al.* (1951)

the calculated density and the constants given by Mandarino (1976), is 1.632. The value of  $2V_x$  measured with an universal stage is nearly  $52^\circ$ . The optical plane is perpendicular to (010) with  $b = Z$  and  $a \sim X$ . The dispersion in the optic axes is  $r < v$  weak. These optical data show an analogy with those quoted for serpierite and devillite (Table 2). Refractive indices as well as the optic axial angle are very similar; the optical sign (-) is the same and clearly related to the stratiform arrangement of

atoms in the three structures. However, the optical orientation and the dispersion in the optical axes of devillite differ from serpierite. From this point of view campigliaite follows the behavior of devillite. The only noticeable difference between devillite and campigliaite lies in the absence of an evident pleochroism in the latter.

Campigliaite crystals are elongated [010] and flattened {100}. It was not possible to measure interfacial angles.

## II. Crystal structure

CESARE SABELLI

*CNR Centro di Studio per la Mineralogia e la Geochimica dei sedimenti  
Istituto di Mineralogia dell'Università  
Via La Pira 4, 50121 Firenze, Italy*

### Experimental and twinning

The search for a crystal suitable for X-ray data collection was laborious, because all the crystals tested were multiple crystals. After many trials a very thin (100) tabular crystal was chosen. Preliminary X-ray Weissenberg photographs showed that it consists of two individuals, almost in the same crystallographic orientation. Furthermore these individuals are affected by polysynthetic twinning with (100) as the twin plane. The larger individual was used for intensity data collection on a Philips PW-1100 four-circle diffractometer (Centro di Cris-

tallografia Strutturale del CNR, Pavia, Italy). A least-squares refinement of 25 high-angle reflections yielded for the unit cell  $a = 21.725(8)$ ,  $b = 6.118(6)$ ,  $c = 11.233(7)\text{Å}$  and  $\beta = 100.40(5)^\circ$  in good agreement with the values obtained by the powder method. Diffraction intensities were collected with graphite monochromated  $\text{MoK}\alpha$  radiation, in the range  $2^\circ < \theta < 25^\circ$ ,  $\omega - 2\theta$  scan technique, integration width of  $1.3^\circ$  and scan speed of  $0.025^\circ/\text{sec}$ . Intensities were corrected for Lorentz and polarization effects. Because of the small size of the crystal the absorption correction was not applied; howev-

er, a partial compensation was achieved by averaging the intensities of equivalent reflections.

Figure 4 reports the reflection population due to the whole crystal and referred to reciprocal lattice levels with  $k = 2n$  (levels with  $k = 2n + 1$  can be represented by a similar scheme with  $h$ -odd lattice points occupied instead of  $h$ -even ones). Only the reflections from 0 to 8 for  $h$  index and from 0 to 9 for  $l$  index are represented. Intensity data could be sorted into two categories; the first one containing the clearly well-separated reflections (with  $l = 1, 2, 4, 7, 10$ ) and the second, about twice as numerous, grouping more or less overlapped reflections (with  $l = 0, 3, 5, 6, 8, 9, 11, 12, 13$ ). From the intensities of non-superimposed reflections of the first set the relative volumes of the two members of the twin were easily computed. The knowledge of the volume ratio ( $A/B = 2.2$ ) allowed the composite intensities of the second set to be subdivided into the intensities of A and B components. Some uncertainties occur in determining the intensities of the partially overlapped reflections; for these a scale

factor proportional to the overlap degree was applied.

Out of the 2528 measured intensities a total of 1426 independent reflections were obtained by averaging all the equivalent ones and by correcting, as shown above, for the twin. Of these data only 689 observations were judged to be actually measured according to the criterion  $F_o > 5\sigma(F_o)$ , with  $\sigma$  derived from counting statistics, and were included in the subsequent least-squares refinement. The systematic extinctions ( $hkl$ ,  $h + k = 2n + 1$ ) are consistent with the space groups  $C2$ ,  $Cm$  and  $C2/m$ ; on the basis of structural considerations the space group  $C2$  was assigned and found to be satisfactory for the refinement.

On the whole, the data set used for the structure analysis is recognized to be of inferior quality because: (1) the crystal used for data collection is tiny and hence the number of "unobserved" intensities is large; (2) the twinning affecting this crystal makes it difficult to assign the right intensity to the reflections partially superimposed; (3) in addition, this crystal is a double crystal and the diffractions due to one individual often interfere with those of the other. The structure refinement of campigliaite could undoubtedly be improved if an untwinned true single crystal, large enough to yield a high ratio of observed to unobserved reflections, could be found.

### Crystal structure analysis

As shown in Table 2 there is a strong similarity between campigliaite, devillite, and serpierite in regard to the chemical formula, the optical data and cell dimensions. In addition, the crystal habit and the strongest lines of the powder pattern of campigliaite are comparable with those of devillite and serpierite (Faraone *et al.*, 1967). Therefore, the starting point for the structure solution was the hypothesis that a continuous copper-oxygen sheet characterizes campigliaite as well as devillite and serpierite (Sabelli and Zanazzi, 1968, 1972).

The copper-oxygen sheet, parallel to (100), can be located at  $x=0$  and  $1/2$  (containing two fold axes) or at  $x=1/4$  and  $3/4$  (containing screw axes), in the space groups  $C2$  and  $C2/m$ . On the other hand, the space group  $Cm$ , as well as  $C2/m$ , is possible because the Cu and O atoms in the sheet show an arrangement consistent with the presence of a mirror perpendicular to the sheet itself.

As in serpierite and devillite, in campigliaite the copper ions and the oxygen atoms of the copper

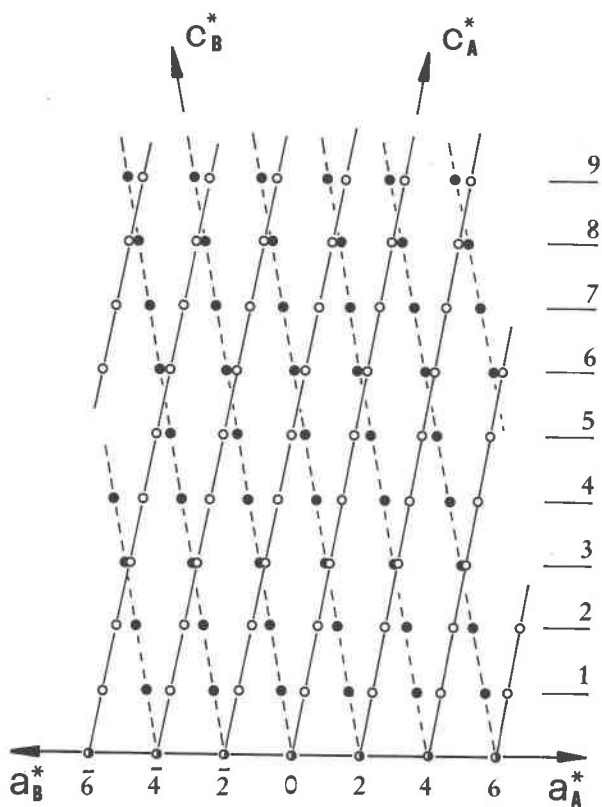


Fig. 4. A  $k$ -even layer of the reciprocal lattice of the twinned campigliaite. The open circled lattice belongs to the A member and the black-dotted lattice to the B member of the twin.

Table 3. Fractional atomic coordinates and isotropic thermal parameters ( $\text{\AA}^2$ )

Atom	x	y	z	B eq.
Cu (1)	0.2488 (5)	0.528 (2)	-0.0001 (10)	1.39
Cu (2)	0.2590 (3)	0.780 (2)	0.2511 (6)	1.63
Cu (3)	0.2596 (3)	0.258 (2)	0.2554 (6)	1.21
Cu (4)	0.2497 (5)	0.518 (2)	0.5013 (10)	1.36
Mn	0.5331 (4)	0.437 (2)	0.2612 (7)	2.41
S (1)	0.1151 (6)	0.205 (2)	0.0556 (9)	2.59
S (2)	0.3930 (6)	0.701 (2)	0.4800 (11)	1.20
O (1)	0.306 (1)	0.023 (8)	0.187 (3)	1.85
O (2)	0.291 (1)	0.541 (8)	0.167 (3)	1.59
O (3)	0.181 (1)	0.267 (7)	0.074 (3)	3.06
O (4)	0.195 (1)	0.736 (7)	0.061 (3)	2.40
O (5)	0.296 (2)	0.255 (6)	0.459 (3)	2.04
O (6)	0.327 (1)	0.755 (6)	0.445 (3)	2.63
O (7)	0.219 (1)	0.026 (7)	0.311 (4)	1.82
O (8)	0.218 (2)	0.558 (6)	0.316 (3)	1.79
O (9)	0.087 (2)	0.104 (6)	-0.065 (3)	4.86
O (10)	0.108 (1)	0.033 (6)	0.145 (3)	4.34
O (11)	0.083 (1)	0.416 (6)	0.069 (4)	3.89
O (12)	0.402 (2)	0.518 (7)	0.570 (3)	8.12
O (13)	0.416 (2)	0.586 (7)	0.372 (3)	4.58
O (14)	0.423 (1)	0.914 (6)	0.520 (3)	1.45
O (15)	0.500 (2)	0.789 (6)	0.236 (3)	2.73
O (16)	0.573 (2)	0.118 (6)	0.277 (3)	2.68
O (17)	0.471 (2)	0.158 (6)	0.356 (3)	4.83
O (18)	0.484 (2)	0.167 (6)	0.110 (3)	5.62
H (1)	0.355	0.030	0.200	4.00
H (2)	0.333	0.557	0.135	4.00
H (3)	0.158	0.630	0.064	4.00
H (4)	0.330	0.341	0.504	4.00
H (5)	0.182	0.028	0.256	4.00
H (6)	0.168	0.579	0.298	4.00
H (7)	0.470	0.732	0.177	4.00
H (8)	0.472	0.726	0.280	4.00
H (9)	0.576	0.047	0.345	4.00
H (10)	0.576	0.050	0.208	4.00
H (11)	0.453	0.077	0.410	4.00
H (12)	0.454	0.301	0.362	4.00
H (13)	0.460	0.313	0.095	4.00
H (14)	0.452	0.083	0.050	4.00

For non hydrogen atoms B eq.'s are the equivalent values after Hamilton (1959).

coordination polyhedra should have particular positions: it is very likely that they contribute almost entirely to the structure factors of  $k$ -even reflections. In order to avoid the contribution of these reflections, which are the strongest ones also, a Patterson synthesis with  $k$ -odd reflections only was computed. This map gives information about Mn-Mn, Mn-S and S-S distances. On the basis of Mn and S positions in the structure the most likely space group is  $C2$  rather than  $C2/m$  or  $Cm$ , because no important vectors due to mirror symmetry are evident in the Patterson map. At this point the Mn atom can be located approximately half way be-

tween the two fold axes, and consequently the copper-oxygen sheet, to which the  $\text{SO}_4$  groups are attached, is on the screw axes.

From this model all the non-hydrogen atomic positions were determined by reiteration of structure-factor and electron-density calculation. During several full-matrix isotropic ( $R = 0.18$ ) and anisotropic ( $R = 0.13$ ) cycles of refinement the temperature factors for the oxygen atoms, especially those belonging to Mn and S polyhedra, were observed to increase and to decrease arbitrarily. Also the shifts in the atomic positions were often statistically insignificant. Towards the end of the refinement a final electron-density difference synthesis was computed, but attempts to locate the hydrogen atoms from this map failed. The hydrogen atoms were placed in geometrically expected positions, at about  $1/3$  of the donor-acceptor distances, and were included in structure factor calculations but not refined. They

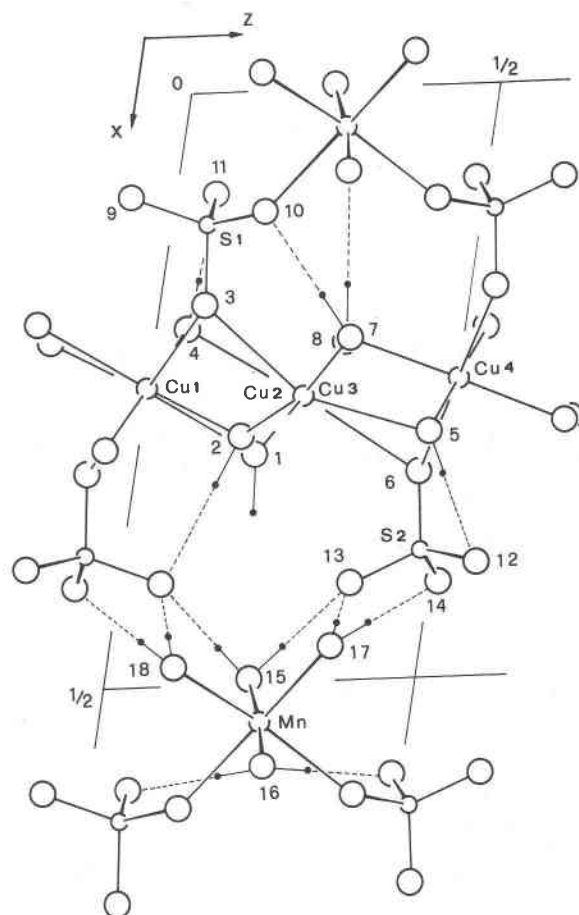


Fig. 5 The structure of campigliaite projected down the  $b$  axis. Solid circles indicate hydrogen atoms and dashed lines hydrogen bonds.

Table 5. Selected interatomic distances (Å) and angles (°)

Cu(1)-O(4)	1.94	Mn-O(16)	2.13	Cu(1)-Cu(2)	3.19
Cu(1)-O(2)	1.93	Mn-O(12,6)	2.20	Cu(1)-Cu(3)	3.28
Cu(1)-O(1,10)	2.22	Mn-O(15)	2.27	Cu(1)-Cu(1,10)	3.06
Cu(1)-O(4,12)	2.34	Mn-O(10,3)	2.34	Cu(1)-Cu(3,10)	3.17
Cu(1)-O(3,10)	2.37	Mn-O(18)	2.47	Cu(1)-Cu(2,12)	3.18
Cu(1)-O(3)	2.42	Mn-O(17)	2.53	Cu(2)-Cu(3)	3.19
				Cu(2)-Cu(4)	3.27
				Cu(2)-Cu(3,1)	2.92
Cu(2)-O(8)	1.85	S(1)-O(3)	1.46	Cu(2)-Cu(4,9)	3.18
Cu(2)-O(7,1)	1.92	S(1)-O(10)	1.48	Cu(3)-Cu(4)	3.23
Cu(2)-O(2)	1.94	S(1)-O(11)	1.49	Cu(3)-Cu(4,11)	3.14
Cu(2)-O(1,1)	2.01	S(1)-O(9)	1.51		
Cu(2)-O(6)	2.40				
Cu(2)-O(4)	2.34	O(3)-S(1)-O(10)	108	O(1)-H(1)	
		O(3)-S(1)-O(11)	103	O(2)-H(2)...O(9,10)	3.10
		O(3)-S(1)-O(9)	117	O(4)-H(3)...O(11)	3.14
Cu(3)-O(7)	1.84	O(10)-S(1)-O(11)	116	O(5)-H(4)...O(12)	2.90
Cu(3)-O(1)	1.99	O(10)-S(1)-O(9)	104	O(7)-H(5)...O(10)	2.76
Cu(3)-O(2)	2.17	O(11)-S(1)-O(9)	109	O(8)-H(6)...O(16,5)	3.12
Cu(3)-O(8)	2.21				
Cu(3)-O(5)	2.29			O(15)-H(7)...O(9,10)	2.69
Cu(3)-O(3)	2.41	S(2)-O(6)	1.45	O(15)-H(8)...O(13)	2.87
		S(2)-O(14)	1.49	O(9,10)-O(15)-O(13)	76
		S(2)-O(12)	1.50		
		S(2)-O(13)	1.56	O(16)-H(9)...O(14,8)	2.59
Cu(4)-O(5,9)	1.86			O(16)-H(10)...O(11,4)	2.69
Cu(4)-O(5)	2.00	O(6)-S(2)-O(14)	104	O(14,8)-O(16)-O(11,4)	123
Cu(4)-O(8)	2.08	O(6)-S(2)-O(12)	111		
Cu(4)-O(7,9)	2.09	O(6)-S(2)-O(13)	109	O(17)-H(11)...O(14,2)	2.72
Cu(4)-O(6)	2.39	O(14)-S(2)-O(12)	117	O(17)-H(12)...O(13)	2.90
Cu(4)-O(6,11)	2.47	O(14)-S(2)-O(13)	116	O(14,2)-O(17)-O(13)	104
		O(12)-S(2)-O(13)	100		
				O(18)-H(13)...O(9,10)	3.08
				O(18)-H(14)...O(11,12)	2.73
				O(9,10)-O(18)-O(11,12)	101

The equivalent positions (referred to Table 2) are designated by the second number in parentheses and are: (1)= $x, 1+y, z$ ; (2)= $x, -1+y, z$ ; (3)= $1/2+x, 1/2+y, z$ ; (4)= $1/2+x, -1/2+y, z$ ; (5)= $-1/2+x, 1/2+y, z$ ; (6)= $1-x, y, 1-z$ ; (7)= $1-x, y, -z$ ; (8)= $1-x, -1+y, 1-z$ ; (9)= $1/2-x, 1/2+y, 1-z$ ; (10)= $1/2-x, 1/2+y, -z$ ; (11)= $1/2-x, -1/2+y, 1-z$ ; (12)= $1/2-x, -1/2+y, -z$ .

O-Cu-O angles range from 70° to 113° between adjacent oxygens, and from 154° to 179° between opposite oxygens. O-Mn-O angles range from 64° to 120° and from 151° to 174°.

The standard deviations are 0.01 to 0.05 Å for distances and 1.2° to 1.7° for angles

were assigned isotropic thermal parameters of  $4.0\text{Å}^2$ . The last cycle of refinement resulted in a final conventional  $R$  index of 0.124 for the 689 "observed" reflections ( $R = 0.213$  for all data). The scattering factors for all atoms were taken from *International Tables for X-ray Crystallography* (1974, p. 99-101). Positional and isotropic thermal parameters are given in Table 3. Anisotropic thermal parameters and observed and calculated structure factors are listed in Tables 3a and 4 respectively.<sup>2</sup>

<sup>2</sup>To receive a copy of Tables 3a and 4, order AM-82-196 and AM-82-197 respectively from the Business Office, Mineralogical Society of America, 2000 Florida Avenue, N. W., Washington, D. C. 20009. Please remit \$1.00 in advance for the microfiche.

### Discussion of the structure

An illustration of the structure of campigliaite is given in Figure 5 and selected bonding dimensions are reported in Table 5. The results confirm the supposed close similarities between campigliaite and the two similar minerals devillite and serpierite. Indeed, the layers of copper-oxygen polyhedra are packed in an essentially identical way, despite the symmetry differences in the three monoclinic space groups. These continuous sheets characterize also the structures of ktenasite,  $(\text{Cu}, \text{Zn})_5(\text{SO}_4)_2(\text{OH})_6 \cdot 6\text{H}_2\text{O}$ , and posnjakite,  $\text{Cu}_4(\text{SO}_4)(\text{OH})_6 \cdot \text{H}_2\text{O}$  (Mellini and Merlino, 1978, 1979). Therefore, from the crystal chemical point of view, campigliaite can be regarded as a new member of the group of the

copper sulfate minerals which feature these atomic slabs.

The low precision of the structure analysis makes a discussion of the observed bond lengths difficult. The environment of the  $\text{Cu}^{2+}$  ions shows the usual Jahn-Teller effect. The other polyhedra in the structure are also distorted. The Mn atom is coordinated by four  $\text{H}_2\text{O}$  molecules and two O atoms from the  $\text{SO}_4$  groups. Bond length and angle variations within the octahedron are relatively wide, with mean Mn-O length of 2.31 Å, substantially longer than the value 2.22 Å expected for  $\text{Mn}^{2+}$  in octahedral coordination (Shannon and Prewitt, 1969). Both  $\text{SO}_4$  groups are linked to the copper-oxygen sheet by a corner. The mean S-O distance (1.49 Å) is longer than the average value (1.473 Å) of well refined structures of hydrated sulfates (Baur, 1964). The scattering of O-S-O angles is wider than usually encountered.

The number of independent water molecules in the structure was assumed to be four, in spite of the result of the chemical analysis because no peak attributable to an additional oxygen atom was present in the Fourier maps. The ratio of the cell volume to the number of oxygen atoms in the cell is  $20.3\text{Å}^3$  when four water molecules are assumed in the formula unit. This is close to the values for devillite and serpierite which are 20.4 and  $20.5\text{Å}^3$  respectively. A volume per oxygen of  $19.3\text{Å}^3$  as derived for  $5\text{H}_2\text{O}$  (and obviously the still lower value for  $6\text{H}_2\text{O}$ )

seems unlikely when compared with the values for devillite and serpierite, and also with the values of 21.2 and  $20.2\text{Å}^3$  calculated for posnjakite and ktenasite.

Unfortunately it is not possible to locate with certainty any of the hydrogen atoms with the data at hand. In addition to the O-O distances reported in Table 5 which are potential hydrogen bonds, there are four more distances, namely O(4)-O(10,1) 2.91 Å, O(7)-O(12,11) 3.15 Å, O(15)-O(16,1) 2.56 Å and O(18)-O(18,7) 2.69 Å, which could be hydrogen bonds. From geometrical considerations and especially on the basis of the balance of valences (Table 6), though this balance is not very satisfactory, the bonds of Table 5 were preferred. Only one hydroxyl hydrogen, H (1), does not seem to be involved in an hydrogen bond, because no distance less than 3.5 Å from O(1) to any oxygen external to the sheet was observed. The electrostatic balance was computed after Brown and Shannon (1973) with data from their Table 1 and the hydrogen bond curve of Donnay and Donnay (1973).

The main significant difference between the structures of devillite and serpierite on one side and campigliaite on the other side lies in the mode of sheet stackings. In devillite and serpierite neighboring sheets, with their  $\text{SO}_4$  appendages, are connected through Ca polyhedra. In campigliaite Mn shares two oxygen atoms of two  $\text{SO}_4$  groups attached to the same sheet; on the opposite side Mn is bonded

Table 6. Electrostatic valence balance

		Cu(1)	Cu(2)	Cu(3)	Cu(4)	Mn	S(1)	S(2)	H-	...H	Sum
O(1)	OH	0.28	0.34	0.44					1.00		2.06
O(2)	OH	0.57	0.41	0.28					0.87		2.13
O(3)		0.19+0.17		0.16			1.63				2.15
O(4)	OH	0.57+0.22	0.15						0.87		1.81
O(5)	OH			0.21	0.60+0.42				0.83		2.06
O(6)			0.13		0.17+0.14			1.71			2.15
O(7)	OH		0.43	0.66	0.33				0.80		2.22
O(8)	OH		0.54	0.25	0.34				0.87		2.00
O(9)							1.38			0.13+0.24+0.13	1.88
O(10)						0.31	1.50			0.20	2.01
O(11)							1.49			0.13+0.22+0.20	2.04
O(12)						0.42		1.48		0.17	2.07
O(13)								1.27		0.18+0.18	1.63
O(14)								1.54		0.26+0.19	1.99
O(15)	Ow					0.35			0.76+0.82		1.93
O(16)	Ow					0.49			0.74+0.78	0.13	2.14
O(17)	Ow					0.20			0.81+0.82		1.83
O(18)	Ow					0.23			0.87+0.80		1.90



to water molecules, which assure the connection with the adjacent sheet only by hydrogen bonds. This difference in the sheet stacking explains the higher water content of campigliaite.

### Acknowledgements

The authors would like to thank S. De Cassai (Miniera di Campiglia SpA) for sampling permission; F. Conticini (Firenze) for his collaboration in the field and laboratory work; L. Giannini and M. Ulivi (Firenze) for their assistance in SEM study; S. Capedri and G. Garuti (Modena) for their collaboration in the analysis with the electron microprobe equipment of the Consiglio Nazionale delle Ricerche, at the Istituto di Mineralogia e Petrografia dell'Università di Modena; A. Kato (Tokyo) for his helpful advice and suggestions.

### References

- Baur, W. H. (1964) On the crystal chemistry of salt hydrates. IV. The refinement of the crystal structure of  $\text{MgSO}_4 \cdot 7\text{H}_2\text{O}$  (epsomite). *Acta Crystallographica*, 17, 1361–1369.
- Brown, J. D. and Shannon, R. D. (1973) Empirical bond-strength–bond-length curve for oxides. *Acta Crystallographica*, A29, 266–282.
- Conticini, F., Menchetti, S., Sabelli, C. and Trosti-Ferroni, R. (1980) Minerali di alterazione dei giacimenti a solfuri misti di Campiglia Marittima (Toscana). *Rendiconti della Società Italiana di Mineralogia e Petrologia*, 36, 295–308.
- Donnay, G. and Donnay, J. D. H. (1973) Bond valence summation for borates. *Acta Crystallographica*, B29, 1417–1425.
- Faraone, D., Sabelli, C. and Zanazzi, P. F. (1967) Su due solfati basici idrati: serpierite e devillite. *Accademia Nazionale dei Lincei; Rendiconti della classe di Scienze fisiche, matematiche e naturali*, 43, 369–382.
- Hamilton, W. C. (1959) On the isotropic temperature factor equivalent to a given anisotropic temperature factor. *Acta Crystallographica*, A27, 368–376.
- International Tables for X-ray Crystallography, Vol. IV (1974) Kynoch Press, Birmingham, England.
- Mandarino, J. A. (1976) The Gladstone-Dale relationship. Part I: derivation of new constants. *Canadian Mineralogist*, 14, 498–502.
- Mellini, M. and Merlino, S. (1978) Ktenasite, another mineral with  ${}^2_2 [(\text{Cu}, \text{Zn})_2(\text{OH})_3\text{O}]^-$  octahedral sheets. *Zeitschrift für Kristallographie*, 147, 129–140.
- Mellini, M. and Merlino, S. (1979) Posnjakite:  ${}^2_2 [\text{Cu}_4(\text{OH})_6(\text{H}_2\text{O})\text{O}]$  octahedral sheets in its structure. *Zeitschrift für Kristallographie*, 149, 249–257.
- Nickel, E. H. (1976) New data on woodwardite. *Mineralogical Magazine*, 43, 644–647.
- Palache, C., Berman, H. and Frondel, C. (1951) *Dana's System of Mineralogy*. Wiley, New York.
- Rodolico, F. (1931) Osservazioni cristallografiche sulla ilvaite. *Periodico di Mineralogia*, 2, 122–132.
- Sabelli, C. and Zanazzi, P. F. (1968) The crystal structure of serpierite. *Acta Crystallographica*, B24, 1214–1221.
- Sabelli, C. and Zanazzi, P. F. (1972) The crystal structure of devillite. *Acta Crystallographica*, B28, 1182–1189.
- Shannon, R. D. and Prewitt, C. T. (1969) Effective ionic radii in oxides and fluorides. *Acta Crystallographica*, B25, 925–946.

*Manuscript received, April 16, 1981;  
accepted for publication, September 17, 1981.*